rich2/cjp-cjp/cjp-cjp/cjp99914/cjp0388d14z | xppws | S=3 | 4/8/14 | 5:39 | 4/Color Fig: F1-F5 | Art: cjp-2013-0622 | Input-1st disk, 2nd ??
Pagination not final (cite DOI) / Pagination provisoire (citer le DOI)

NRC Research Press

ARTICLE

Photocurrent analysis of In–Ga–Zn–O (IGZO) film[1]

Ju-Yeon Kim, Kyeong-Min Yu, So-Hyeon Jeong, Eui-Jung Yun, and Byung Seong Bae

Abstract: We investigated the electrical properties of the In–Ga–Zn–O (IGZO) film under light illumination. We measured the photoconductivity of a-IGZO thin film under light illumination with various intensities. We extracted the photoexcitation activation energy and dark relaxation activation energy through extended stretched exponential analysis. Dark relaxation characteristics, which are related to the recombination process, show longer time constant, τ, larger effective activation energy E_{ac}, and lower stretching exponent, β, with wider activation energy bandwidth, Δ_{ac}, than those corresponding to those of photoexcitation. These indicate that recombination takes place more slowly and through more deeply bound activation processes with the broader distribution of activation energies than those corresponding to photogeneration process. The wider distribution for the dark relaxation energy for the higher light intensity suggests that the metastable state distribution is related to the distribution of the oxygen vacancy state, V_o. We also concluded that the usage of the right value of the attempt-to-escape frequency is important to estimate the exact value of E_{ac}.

PACS Nos.: 73.50.Pz, 73.50.–h, 73.61.–r.

Résumé : Nous étudions les propriétés électriques de films de In–Ga–Zn–O (IGZO) sous éclairage lumineux. Nous mesurons la photoconductivité de films minces de a-IGZO sous illumination d'intensité variable. L'analyse étendue par exponentielle étirée nous permet d'extraire l'énergie d'excitation d'activation et l'énergie de relaxation d'activation en obscurité. Les caractéristiques de relaxation en obscurité, qui sont reliées au mécanisme de recombinaison, montrent une plus grande constante de temps, τ, de plus grandes énergies d'activation efficaces, E_{ac}, et de plus faibles exposants d'étirement, β, avec une plus large largeur de bande d'énergie d'activation, Δ_{ac}, que celles correspondant à la photo-excitation. Elles indiquent que la recombinaison se produit plus lentement et via un processus d'activation plus profondément liés avec de plus larges distributions d'énergies d'activation que celles correspondant au procédé de photo-génération. Ajoutons que la plus large distribution de l'énergie de relaxation en obscurité pour des intensités lumineuses plus élevées, suggère que la distribution d'états métastables est reliée à la distribution de l'état V_o lacunaire d'oxygène. Nous concluons aussi que l'utilisation de la bonne valeur de la fréquence des essais-de-fuite est importante pour calculer la bonne valeur de E_{ac}. [Traduit par la Rédaction]

1. Introduction

Nowadays, amorphous In–Ga–Zn–O thin film transistors (a-IGZO TFTs) are getting a lot of attention from many researchers [1–4]. Compared to other devices, such as a hydrogenated amorphous silicon (a-Si:H) TFT or polycrystalline silicon TFT (poly-Si TFT), a-IGZO TFTs have advantages, such as transparency, high mobility, and ease of manufacturing [5, 6]. The disadvantages of a-Si:H TFTs are low mobility (<1 cm^2/Vs) and instability under light illumination and electrical bias stress. Therefore, it is difficult to make large and high resolution displays with a-Si:H TFT.

Poly-Si TFTs have well known advantages, such as a high carrier mobility (>100 cm^2/Vs) and excellent stability. However, the main disadvantages of poly-Si TFTs are short-range nonuniformity and high manufacturing cost. High mobility is essential for making displays with superior resolution [5–8]. The a-IGZO TFT shows higher mobility than a-Si:H TFT. Because oxide TFTs use the same structure as a-Si:H TFTs, which employ a simpler process compared to poly-Si TFTs, the oxide TFT process is as simple as that of a-Si:H TFT, suggesting that oxide TFTs are suitable for large area display with low cost.

However, oxide TFTs are very sensitive to electrical stress and ambient conditions, such as light, temperature, and moisture [6, 9]. Stability issues have been one of the main research themes from the early stage of development in oxide TFTs. Many researches of subgap density of states have been reported for a-IGZO TFTs; however, combined and unified models have not been established yet. The research on single a-IGZO thin films is very limited and based mainly on the research of TFTs, which is complex because of the presence of the gate insulator. Therefore, we investigated the electrical properties of a single IGZO film under light illumination. In this work, the photocurrent of a-IGZO thin films was measured at various intensities and analyzed to investigate the bandgap states.

2. Experiment

An a-IGZO thin film was deposited by sputtering under ambient Ar and O_2. An Al electrode was deposited via thermal evaporation. The thickness of a-IGZO thin films was 100 nm. The width and length of the Al electrodes were 1500 and 100 μm, respectively. To avoid the effect of moisture and other impurities, the measurement was conducted in a vacuum chamber. We measured the photocurrent of a-IGZO thin film under white light illumination at a temperature of 60 °C. The intensities of the light source were 6 and 37 mW/cm^2. The illumination duration was 10 min. For the recovery to the original state after measurement, the sample was annealed for 1 h at a temperature of 180 °C.

Received 22 October 2013. Accepted 27 February 2014.

J.-Y. Kim, K.-M. Yu, S.-H. Jeong, and B.S. Bae. Department of Display Engineering, Hoseo University, Asan-city, Chungnam 336-795, Korea.
E.-J. Yun. Colleage of Green Energy Semiconductor Engineering and Department of System Control Engineering, Hoseo University, Asan-city, Chungnam 336-795, Korea.
Corresponding author: Byung Seong Bae (e-mail: bsbae3@hoseo.edu).

[1]This paper was presented at the 25th International Conference on Amorphous and Nanocrystalline Semiconductors (ICANS25).

Published at www.nrcresearchpress.com/cjp on 4 March 2014.

The photocurrents were measured while the light turned on and off to study the electrical properties of a-IGZO thin films under white light illumination.

3. Results and discussion

The photocurrent of a-IGZO thin film was measured under light intensities of 6.0 and 37 mW/cm^2. As shown in Fig. 1, the increase of the conductivity (σ) was observed while the light was illuminated. Once the light turned off, the conductivity of the a-IGZO thin film was slowly declined. The dark conductivities recovered to their original values after about 12 h at room temperature and about 1 h at 373 K.

In general, conductivity changed immediately after the light turned on or off, indicating the presence of short time constants in the photoconductivity response. On the other hand, in this measurement, during photoexcitation or dark relaxation, conductivity was changing significantly, but at progressively slower rates. In the amorphous state it is general that multiple time constants are involved in the photoresponse; therefore, the photoconductivity change over time, t, can be described by several time constants, τ_i [5]

$$\sigma_{ph}(t) = |\sigma(t) - \sigma_s| = \sum_i \sigma_i e^{-t/\tau_i} \quad (1)$$

where the photoresponse conductivity, σ_{ph}, is the difference between time-dependent conductivity and the saturation conductivity of asymptotic curve σ_s at long times. The photoconductivity was explained by Luo et al. [5] by using the stretched exponential function

$$\sigma_{ph}(t) = \sigma_{ph,0}\exp\left[-\left(\frac{t}{\tau}\right)^{\beta}\right] \quad (2)$$

where $\sigma_{ph,0}$ is the weighing amplitude, τ is the effective time constant, and β is the stretching exponent. τ can be defined as the time when the time-dependent photoconductivity, $\sigma_{ph}(t)$, relaxes to 1/e of its initial value of $\sigma_{ph,0}$.

The activation energy, $E(t)$, and the activation energy bandwidth, Δ_{ac}, were calculated by making use of (3) and (4), respectively [5]

$$E(t) = k_B T \ln(t\nu) \quad (3)$$

$$\Delta_{ac} = 4.6\left(\beta^{-0.81} - 1\right)k_B T \quad (4)$$

where k_B is Boltzmann's constant, T is the sample temperature, t is the time, and ν is the attempt-to-escape frequency. Following other authors [10, 11], E_{ac} (= $E(\tau)$) was calculated from (3) assuming $\nu = 10^{13}$ Hz and $t = \tau$. Equation (4) is a simple empirical equation deduced from Luo et al. [5] and Lee et al. [10], which fits the calculated Δ_{ac} to within 8% and provides a quick way to estimate the Δ_{ac} for any β in the range $0.05 < \beta < 1$. Figure 2a shows a best fit to the photoconductivity data for the sample illuminated with a light intensity of 6.0 mW/cm^2 to estimate the saturation photoconductivity, σ_s, which is the asymptotic conductivity at very long times as mentioned in (1). In the case of the photoexcitation, (1) becomes

$$\sigma_{ph}(t) = \sigma_s - \sigma(t) \quad (5)$$

As shown in Fig. 2a, the photoexcitation data for the 6.0 mW/cm^2 sample were fitted to the stretched exponential function by making use of (2) and (5). The fitting parameters τ and β were obtained from the best fit to the data.

Fig. 1. Comparison of photoexcitation and dark relaxation conductivities on time for the light source powers (6.0 and 37 mW/cm^2).

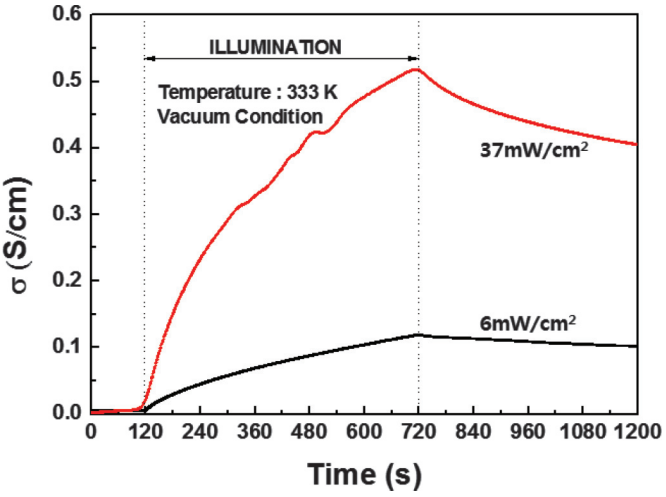

Fig. 2. Stretched exponential fit for the (*a*) photoexcitation, and (*b*) dark-relaxation of the 6.0 mW/cm^2 intensity sample at 333 K as a plot of conductivity, σ, versus time, t.

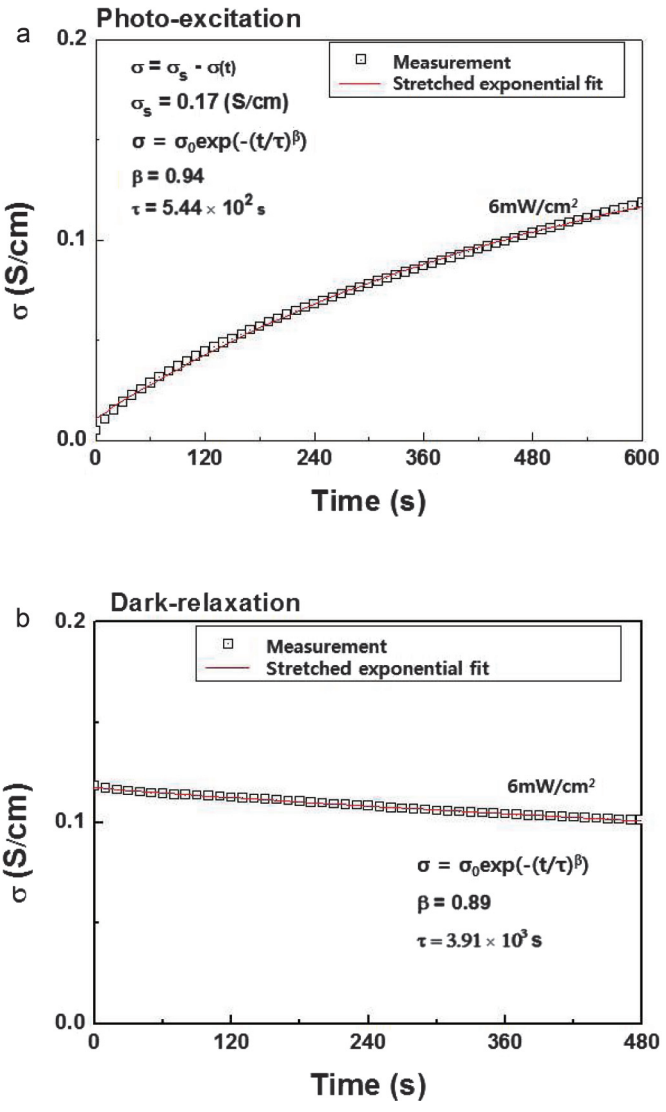

In the case of the dark-relaxation, the saturation conductivity of the dark-relaxation equals zero because the dark conductivities recover their original values as aforementioned. In Fig. 2*b*, the open squares and solid lines show the experimental data and the best fit to the data, respectively. Figure 3 shows dark-relaxation processes for the samples illuminated with the 37 mW/cm² intensity. We obtained fitting parameters for all the measurement data with light power intensities of 6.0 and 37 mW/cm². As shown in Table 1, the values of fitting parameters (β, τ, σ_s) are deduced from best fits to the measured data, and the energy scales for activated behavior, E_{ac}, and Δ_{ac} are derived from inverse Laplace transform analysis of these stretched exponentials [5].

The characteristic of conductivity of a-IGZO thin film versus time as a function of temperature was measured for the light source power of 6 mW/cm² and is shown in Fig. 4. As can be seen, the recovery rate is faster for the higher temperature case. By using the result in Fig. 4 and the same method employed in Figs. 2*b* and 3*b*, we obtained the fitting τ values. Figure 5 shows the temperature-dependence of the τ values for dark-relaxation processes obtained from Fig. 4. We also extracted the activation energy, E_{ac}, from the result of Fig. 5 by making use of

$$\tau = \tau_0 \exp\left(\frac{E_{ac}}{k_B T}\right) \quad (6)$$

where τ is the effective time constant, k_B is Boltzmann's constant, and T is the sample temperature. The extracted E_{ac} value of 0.71 eV is a little bit different from the value of 1.096 eV calculated from (3) assuming $\nu = 10^{13}$ Hz (see Table 1). Here, we emphasize that the ν value of 1.08×10^7 Hz extracted from Fig. 5 is much lower than 10^{13} Hz value used in Table 1. Therefore, the usage of the right value of the attempt-to-escape frequency is important to estimate the exact value of the activation energy.

Based on the results from the stretched exponential analysis, we observed that relaxation process occurs through a more deeply bound activation process. Because the larger the activation energy is, the longer the stretched exponential time constant, τ, is, the recovery time of the dark-relaxation is slower than the photoexcitation, that is, the excitation rate is faster than the recovery rate. The relaxation process showed a larger half-maximum bandwidth, Δ_{ac}, and a smaller stretching exponent, β, compared to photoexcitation process, which indicates that the relaxation is related to a process with wider distribution of activation energy.

It has been believed that the increase in the photoconductivity during the photoexcitation is because of the photoinduced increase of the donor state, which is related to the photoionization of oxygen vacancy, V_o^{2+}. Once the light turned off, the current of the a-IGZO thin film was rapidly decreased and then slowly declined, which is attributed to the neutralization of V_o^{2+}. It was reported that the ionized oxygen vacancy (V_o^{2+}) can cause photocarriers and metastability [9, 11–14]. The long relaxation time originating from this metastability is not fully understood. The hole-mediated formation of the metastable peroxide defects was also suggested as an origin of the metastability by light illumination and bias stress [15]. They suggest that the metastable activation energy for the structural recovery is found to be 0.97 eV, which is similar to the activation energy of 1.1 eV for dark relaxation observed in this study.

In Table 1, the dependence of β and Δ_{ac} on light power indicates the larger distribution of activation energies for higher light power. That is, the metastable recovery barrier distribution becomes wider for the higher light power. The oxygen vacancy, which has some energy distribution below the Fermi level is ionized by the illuminated light. The higher power causes the wider distribution of ionized vacancy level, which results in the variation of the metastable defects. This means that the vacancy energy

Fig. 3. Stretched exponential fit for the (*a*) photoexcitation and (*b*) dark-relaxation of the 37 mW/cm² intensity sample at 333 K as a plot of conductivity σ versus time t.

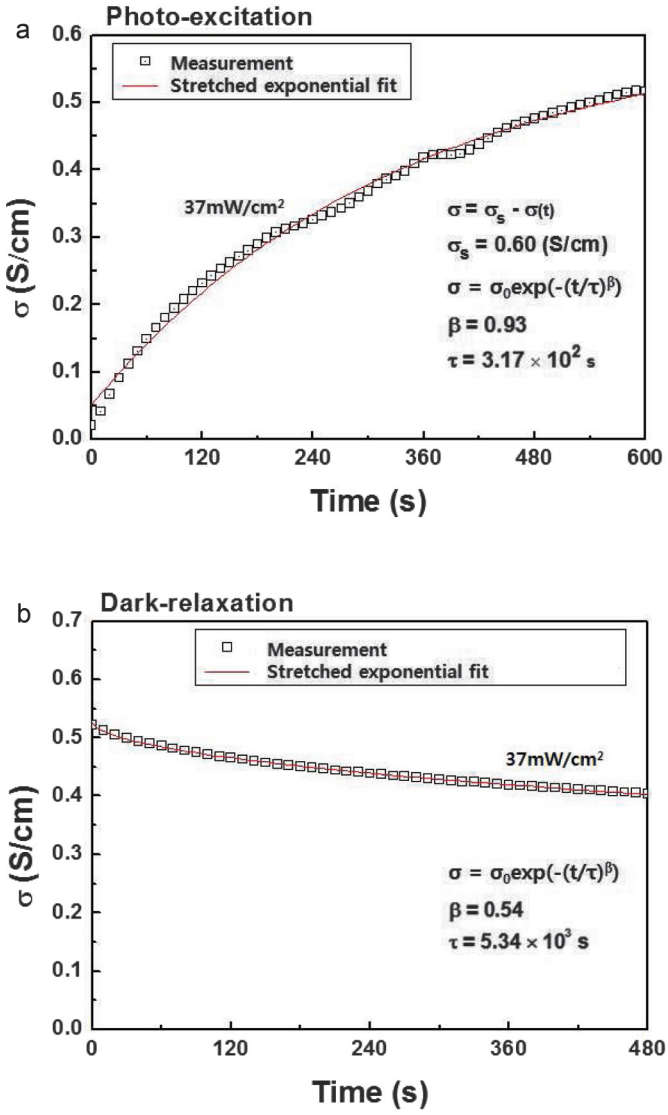

state before the ionization results in a different defect level, which contributes to the slow dark relaxation of conductivity [15]. In this paper, the transient photocurrent response during light illumination and the dark relaxation were investigated for the a-IGZO thin films. According to the standard knowledge in the area of photoconductivity in disordered semiconductor materials [16], transient photoconductivity of photoexcitation and dark relaxation are described by the multiple-trapping model whereby the photoinduced carrier generation and the trap-controlled recombination play a key role. On the other hand, much recent research reports that the oxygen vacancy plays an important role in a-IGZO thin films exposed with light illumination. We believe that the oxygen vacancies can act as deep trap centers and donors when ionized to control transient photocurrent response during light illumination and the dark relaxation.

4. Conclusion

We have investigated the effect of electrical properties of a-IGZO thin films under light Illumination. The magnitude of the photoconductivity increases with increasing illuminated light in-

Table 1. Summary of stretched exponential analysis.

	Photoexcitation					Dark-relaxation				
Intensity (mW/cm^2)	β	τ (s)	σ_s (S/cm)	E_{ac} (eV)	Δ_{ac} (eV)	β	τ (s)	σ_s (S/cm)	E_{ac} (eV)	Δ_{ac} (eV)
6.0	0.94	5.44×10^2	0.17	1.039	0.007	0.89	3.91×10^3	0	1.096	0.013
37	0.93	3.17×10^2	0.60	1.024	0.008	0.54	5.34×10^3	0	1.105	0.085

Note: The values of parameters (β, t, σ_s) are deduced from best fits to the data, and the energy scales for activated behavior, E_{ac}, and Δ_{ac} are derived from inverse Laplace transform analysis of these stretched exponentials.

Fig. 4. Comparison of photoexcitation and dark relaxation conductivities with time as a function of temperature for the light source power of 6 mW/cm^2.

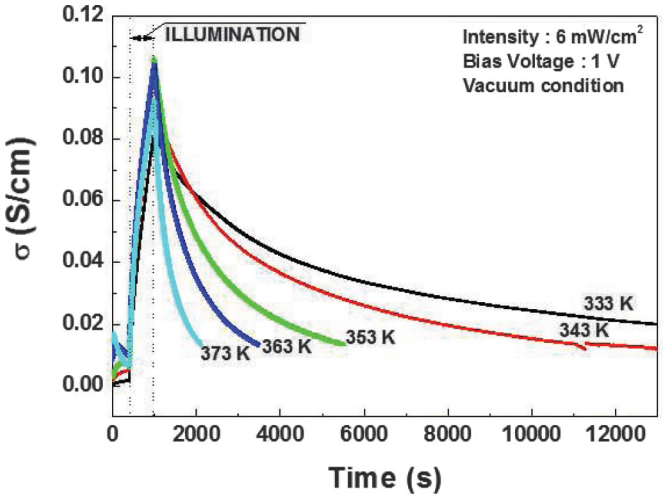

Fig. 5. Temperature-dependence of the fitting τ values for dark relaxation processes obtained from Fig. 4. The activation energy, E_{ac}, was estimated using (6).

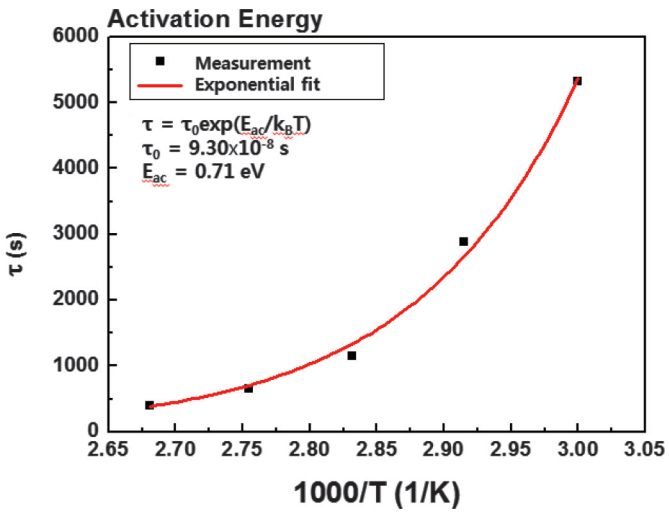

tensity. The stretched exponential analysis was found to describe well both the photoexcitation and dark relaxation characteristics. This suggests that stretched exponential fitting plays an important role in studying the energy distribution of activation processes for both excitation and relaxation. Dark relaxation characteristics, which are related to the recombination process, show longer time constant, τ, larger effective activation energy, E_{ac}, and lower stretching exponent, β, with wider activation energy bandwidth, Δ_{ac}, than those corresponding to photoexcitation ones. These indicate that recombination takes place more slowly and through a more deeply bound activation processes with the broader distribution of activation energies than those corresponding to photogeneration process. We believe that the increase in the photoconductivity during the photoexcitation is principally because of the photoinduced increase in the donor electron density, which is related to the photoionization of oxygen vacancies, V_o^{2+}. Once the light turned off, the current of a-IGZO thin film was rapidly decreased and then slowly declined, which is attributed to the neutralization of V_o^{2+}. And the wider distribution for the dark relaxation energy for the higher light intensity suggests that the metastable state distribution is related to the distribution of the oxygen vacancy state, V_o. We also concluded that the usage of the right value of the attempt-to-escape frequency is important to estimate E_{ac}.

Acknowledgement

This work was supported by the Industrial Strategic Technology Development Program (grant No. 10041596, Development of core technology for TFT free active matrix addressing color electronic paper with day and night usage), funded by the Ministry of Trade, Industry and Energy (MI, Korea).

References

1. K. Nomura, H. Ohta, A. Takagi, T. Kamiya, M. Hirano, and H. Hosono. Nature, **432**, 488 (2004). doi:10.1038/nature03090. PMID:15565150.
2. J.S. Park, W.-J. Maeng, H.-S. Kim, and J.-S. Park. Thin Solid Films, **520**, 1679 (2012). doi:10.1016/j.tsf.2011.07.018.
3. S.H. Ko Park, M. Ryu, S. Yang, S.M. Yoon, and C.S. Hwang. J. Inf. Display, **11**, 113 (2010). doi:10.1080/15980316.2010.9656256.
4. D.-H. Cho, S.-H.K. Park, S. Yang, C.-W. Byun, J. Shin, K.I. Cho, M.K. Ryu, S.M. Chung, W.-S. Cheong, S.-M. Yoon, and C.-S. Hwang. J. Inf. Display, **10**, 137 (2009). doi:10.1080/15980316.2009.9652097.
5. J. Luo, A.U. Adler, T.O. Mason, D.B. Duchholz, R.P.H. Chang, and M. Grayson. J. Appl. Phys. **113**, 153709 (2013). doi:10.1063/1.4795845.
6. T. Kamiya, K. Nomura, and H. Hosono. Technol. Adv. Mater. **11**, 044305 (2010). doi:10.1088/1468-6996/11/4/044305.
7. H. Yabuta, M. Sano, K. Abe, T. Aiba, T. Den, H. Kumomi, K. Nomura, T. Kamiya, and H. Hosono. Appl. Phys. Lett. **89**, 112123 (2006). doi:10.1063/1.2353811.
8. H. Hosono. J. Non-Cryst. Solids, **352**, 851 (2006). doi:10.1016/j.jnoncrysol.2006.01.073.
9. B. Ryu, H.-K. Noh, E.-A. Choi, and K.J. Chang. Appl. Phys. Lett. **97**, 022108 (2010). doi:10.1063/1.3464964.
10. D.H. Lee, K.-I. Kawamura, K. Nomura, T. Kamiya, and H. Hosono. Electrochem. Solid-state. Lett. **13**, H324 (2010). doi:10.1149/1.3460302.
11. H. Oh, S.-M. Yoon, M.K. Ryu, C.-S. Hwang, S. Yang, and S.-H.K. Park. Appl. Phys. Lett. **97**, 183502 (2010). doi:10.1063/1.3510471.
12. H.C. Oh, S.M. Yoon, M.K. Ryu, C.S. Hwang, S.H. Yang, and S.-H.K. Park. Appl. Phys. Lett. **98**, 033504 (2011). doi:10.1063/1.3540500.
13. M.D.H. Chowdhury, P. Migliorato, and J. Jang. Appl. Phys. Lett. **97**, 173506 (2010). doi:10.1063/1.3503971.
14. H.-K. Noh, K.J. Chang, B. Ryu, and W.-J. Lee. Phys. Rev. B, **84**, 115205 (2011). doi:10.1103/PhysRevB.84.115205.
15. H.-H. Nahm, Y.-S. Kim, and D.H. Kim. Phys. Status Solidi B, **249**, 1277 (2012). doi:10.1002/pssb.201147557.
16. M.S. Iovu, S.D. Shutov, V.I. Arkhipov, and G.J. Adriaenssens. J. Non-Crys. Solids, **299–302**, 1008 (2002). doi:10.1016/S0022-3093(01)01067-5.